Submitted to Physical Review Letters, September 10, 1993.

Evidence for Correlated Changes in the Spectrum and Composition of Cosmic Rays at Extremely High Energies

D.J. Bird,[1] S.C. Corbató,[3] H.Y. Dai,[3] B.R. Dawson,[2] J.W. Elbert,[3] T.K. Gaisser,[5]
K.D. Green,[3,4] M.A. Huang,[3] D.B. Kieda,[3] S. Ko,[3] C.G. Larsen,[3] E.C. Loh,[3] M. Luo,[3],
M.H. Salamon,[3] J.D. Smith,[3] P. Sokolsky,[3] P. Sommers,[3] T. Stanev,[5]
J.K.K. Tang,[3] S.B. Thomas,[3] S. Tilav [5,6]

[1] *Department of Physics, University of Illinois at Urbana-Champaign, Urbana, IL 61801 USA*
[2] *Department of Physics and Mathematical Physics, University of Adelaide, Adelaide, South Australia 5005 Australia*
[3] *High Energy Astrophysics Institute,*
Department of Physics, University of Utah, Salt Lake City UT 84112 USA
[4] *Present address: Department of Physics, The University of Michigan, Ann Arbor, MI 48109 USA*
[5] *Bartol Research Institute, University of Delaware, Newark DE 19716*
[6] *Present address: Department of Physics, University of Wisconsin, Madison, WI 53706 USA*

Abstract

The Utah Fly's Eye detector has revealed a change in the cosmic ray composition which is correlated with structure in the all-particle energy spectrum. The data can be fit by a simple model of a steep power law spectrum of heavy nuclei which is overtaken at high energies by a flatter spectrum of protons. The transition occurs near $10^{18.5}$ eV. Anisotropy is not detected, so the high-rigidity particles above the transition energy do not originate in the disk of the Galaxy. An outstanding event of 3×10^{20} eV implies that the highest energy particles originate in the contemporary era of the universe.

The acceleration of extremely high energy cosmic rays (i.e. greater than 10^{17} eV) has puzzled experimentalists and theorists for decades. The energy spectrum, the chemical composition, and the arrival directions of these particles are clues to this mystery and are the only constraints on theories of their origins.

The detection of these extremely high energy cosmic rays is necessarily indirect because of the extremely low flux. The Earth's atmosphere makes their low flux detectable by converting the cosmic ray primaries into extensive air showers of various secondary particles. The Fly's Eye, a detector designed to collect the atmospheric nitrogen fluorescence light produced by air shower particles, is the only detector capable of measuring longitudinal shower developments individually, thus allowing a direct estimation of each shower's primary energy and the atmospheric depth where it reaches maximum size.

The details of the Fly's Eye experiment have been described in earlier papers[1,2]. Briefly, the Fly's Eye detector began full operation in 1981 at Dugway, Utah (40^oN, 113^oW, atmospheric depth 860 g cm^{-2}). The original detector, Fly's Eye I, consists of 67 spherical mirrors of 1.5 m diameter, each with 12 or 14 photomultipliers at the focus. The mirrors are arranged so that the entire night sky is imaged, with each phototube viewing a hexagonal region of the sky 5.5 degrees in diameter. In 1986 a second detector (Fly's Eye II) 3.4 km away came into full operation. Fly's Eye II consists of 36 mirrors of the same design. This detector only views the half of the night sky in the direction of Fly's Eye I. Fly's Eye II can operate as a stand alone device or in conjunction with Fly's Eye I for a stereo view of some showers.

The energy spectrum derived from the Fly's Eye stereo data exhibits remarkable structure (cf. Fig.1). Near the Fly's Eye energy threshold, the spectral index agrees with measurements by experiments in the region above the spectrum's "knee"[3]. The spectrum becomes steeper right after $10^{17.6}$ eV and flattens after $10^{18.5}$ eV. The change in the spectral slope forms a dip centered at $10^{18.5}$ eV. (A spectral flattening near this energy has been observed also by other experiments and is sometimes called the "ankle" of the cosmic ray spectrum. Some evidence for a dip preceding the ankle has also been reported by other groups[4,5].) We divided our stereo energy spectrum into three energy ranges determined by eye and fit them to a power law spectrum in each region. Table 1 shows the normalization and the slope within each region, as well as an overall single power law fit. To show the significance of the dip, the expected number of events based on the best fit to the overall spectrum (renormalized to the observed number of events at $10^{17.6}$ eV) is compared to the actual observed number. The expected number of events between $10^{17.6}$ eV and $10^{19.6}$ eV is 5936.3, and the observed number is 5477. The significance of this deficit is 5.96 σ. To show the significance of flattening above $10^{18.5}$ eV, we use the normalization and slope from a total fit up to $10^{18.5}$ eV (shown in Fig.1 as a dotted line). The total number of observed events above this energy is 281 while the expected number would be 230, which is a 3.4σ excess. The excess is even more pronounced (5.2σ excess over an expected 205.9 events) if the spectrum from $10^{17.6}$ to $10^{18.5}$ eV is used to calculate the expectation. The energy resolution over this region is approximately constant, so the spectral structure cannot be attributed to resolution effects[6]. The raw event distribution also shows a dip at the same energy.

The monocular data set is much larger than the stereo data set, although shower energies typically have larger uncertainties. Fig. 2 shows the total energy spectrum. Because of the limited energy resolution, the energy spectrum observed by the monocular eye does not show the degree of structure found in the stereo data. Monte Carlo simulations verify that the dip seen in the stereo spectrum is necessarily washed out if the energy resolution is degraded to that of the overall monocular data[6]. The dip is evident in the monocular spectrum if tight cuts are imposed to select only events with highly reliable geometrical reconstructions, but then the statistics are again low. The high statistics overall monocular spectrum is presented here to study the high end of the spectrum. Fig. 2 suggests that the flattened spectrum may extend for only about one energy decade, with a steepening right after $10^{19.7}$ eV. The expected number of events above $10^{19.7}$ eV based on the spectrum between $10^{19.0}$ and $10^{19.7}$ eV is 20.63, but only 10 events were observed. A spectral cutoff at this energy is expected due to pion-producing collisions with microwave photons[7,8], but more statistics are needed to resolve this issue observationally.

On Oct. 15, 1991, the Fly's Eye observed an event at $(3.0^{+0.36}_{-0.54}) \times 10^{20}$ eV. This is the highest energy event ever recorded. Details of the air shower will be presented elsewhere[9]. An event of this energy cannot be of cosmological origin. The travel time from its source is limited to approximately 10^8 years[10,11] due to interactions with the microwave background radiation (or radio photons in the case of a gamma ray[12,13]). Apparently, not all sources are at sufficient distances for photoproduction to cut off the cosmic ray spectrum entirely.

A change in the cosmic ray chemical composition is evident in the energy range where the spectrum exhibits the dip and flattening. In two previous papers, we have discussed the Fly's Eye distribution of shower depths of maximum (X_{max}) as a function of energy[14], and what it says about the composition of cosmic ray primaries[15]. The present results are based on a larger data set due to additional running time and also the use of a more efficient matching and reconstruction algorithm for stereo data. This increase in statistics allows us, for the first time, to examine the composition of cosmic rays near 10^{19} eV. The situation is here summarized by displaying the mean X_{max} as a function of energy in Fig. 3. Also shown in that figure are the expected energy dependences of X_{max} for pure iron or pure proton compositions. It can be seen that the elongation rate (change in mean X_{max} per energy decade) is greater than expected for any fixed composition above $10^{17.5}$ eV. This implies that the composition is growing lighter with increasing energy, going from a heavy composition below $10^{17.5}$ eV to a light composition near 10^{19} eV. The specific expectations in Fig. 3 are based on a QCD Pomeron hadronic model. Unlike the spectrum measurement, the composition determination relies on an interaction model. Although different viable models give somewhat different predictions for the mean proton X_{max} and mean iron X_{max} at a fixed energy, they differ little in their predicted elongation rates. As a result, the inference of a changing composition is more robust than the composition determination itself at any fixed energy.

The measured elongation rate agrees quantitatively with what is expected for a transition from a pure iron component below the ankle to a pure proton component above the ankle, in the following sense: We first note that the spectrum can be fitted by the superposition of a steeply falling power law and a flatter power law which dominates above the ankle (cf. Fig. 4). Having determined the spectral indices and normalizations for those two components using only the all-particle spectrum, we compute the expected mean X_{max} (at each energy) assuming the steep component is purely iron and the flatter component is purely protons. The energy dependence of the mean X_{max} computed from this simple two component model matches remarkably well the observed energy dependence as shown in Fig. 3. This two component model is likely an oversimplification of reality, but it conveniently summarizes the observed trends.

Besides the energy spectrum and composition, the arrival directions of cosmic rays should be a clue to the origins of these particles despite the presence of magnetic fields in the Galaxy. A proton of 10^{18} eV energy has an orbit of 1 kpc diameter in the 2.2 μG galactic magnetic field, so the orbit size is comparable to the thickness of the galactic magnetic disk. Analyses of Fly's Eye arrival directions have so far yielded no statistically significant evidence of large scale anisotropy[16,17]. The approximate isotropy can be reconciled with sources in the galactic disk if the particles are the highly charged nuclei indicated by the composition results near $10^{17.5}$ eV. For the light composition at the highest energies, however, the cosmic ray intensity should be highly anisotropic if it originates in the galactic disk. The absence of detectable anisotropy supports the view that the spectral flattening and changing composition signify a transition to cosmic rays of extragalactic origin (although acceleration within a large galactic halo cannot be excluded).

Taken together, the Fly's Eye results on the cosmic ray energy spectrum, chemical composition, and arrival directions strongly suggest a dramatic transition near $10^{18.5}$ eV to a population of different origin. The higher energy particles are lighter than the lower energy population. The lack of detectable anisotropy implies that the higher energy component does not originate in the galactic disk. The detection of an air shower of 3×10^{20} eV means that the highest energy cosmic rays are not relics from the early universe, and not all of the sources are extremely distant.

Acknowledgements

We would like to acknowledge the earlier contributions of R.M.Baltrusaitis, H.Bergeson, R.Cady, R.Cooper, B.L.Emerson, B.Fick, P.R.Gerhardy, D.Liebing, Y.Mizumoto and D.Steck to this experiment. In particular, we would like to thank G.Cassiday for his innumerable contributions to the development of the air fluorescence technique. We are indebted to Colonels Frank Cox and James King and the staff of the Dugway Proving Grounds for their continued cooperation and assistance. This work has been supported in part by the National Science Foundation (grants PHY–91–00221 at Utah and PHY–92–20990 at Bartol) and the U.S. Department of Energy (grant FG02–91ER40677 at Illinois and grant FG02–91ER40626 at Bartol).

Table 1. Spectral slopes and normalizations of J(E) ($m^{-2}sr^{-1}s^{-1}eV^{-1}$)

Energy range (eV)	Power index	log($normalization$)	Normalized at
$10^{17.3} - 10^{19.6}$	-3.18 ± 0.01	-29.593	$10^{18}eV$
$10^{17.3} - 10^{17.6}$	-3.01 ± 0.06	-29.495	$10^{18}eV$
$10^{17.6} - 10^{18.5}$	-3.27 ± 0.02	-29.605	$10^{18}eV$
$10^{18.5} - 10^{19.6}$	-2.71 ± 0.10	-32.623	$10^{19}eV$

References

1. R. M. Baltrusaitis *et al.*, Nuclear Instruments and Methods **A240**, 410 (1985).
2. G. L. Cassiday, Ann. Rev. Nucl. Part. Sci. **35**, 321 (1985).
3. M. Nagano *et al.*, J. Phys. G.: Nucl. Part. Phys. **10**, 1295 (1984).
4. M. A. Lawrence, R. J. O.Reid, and A. A. Watson, J. Phys. G.: Nucl. Part. Phys. **17**, 733 (1991).
5. M. Nagano *et al.*, J. Phys. G.: Nucl. Part. Phys. **18**, 423, (1992).
6. D. J. Bird *et al.*, "Cosmic Ray Energy Spectrum Observed by the Fly's Eye," (to appear in Ap. J.).

7. K. Greisen, Phys. Rev. Lett. **16**, 748 (1966).

8. G. T. Zatsepin and V. A. Kuzmin , Sov. Phys. JETP Lett. **4**, 78 (1966).

9. In preparation

10. J. L. Puget, F. W. Stecker, and J. H. Bredekamp, Ap. J. **205**, 638 1976.

11. C. T. Hill and D. N. Schramm, Phys. Rev. **D31**, 564 (1985).

12. R. J. Gould and G. P. Schreder, Phys. Rev. **155**, 1408, (1967).

13. J. Wdowczyk, W. Tkaczyk, and A. W. Wolfendale, J. Phys. **A5**, 1419 (1972).

14. G. L. Cassiday *et al.*, Ap. J. **356**, 669 (1990).

15. T. K. Gaisser *et al.*, Physical Review **D47**, 5, 1919 (1993).

16. G. L. Cassiday *et al.*, Ap. J. **351**, 454, (1990).

17. D. J. Bird *et al.*, in *Proceedings of the 23rd International Cosmic Ray Conference, Calgary, 1993*, Vol 2, p51.

Figure Captions

Figure 1: Fly's Eye stereo differential energy spectrum multiplied by E^3. Points: data. Dashed line: best fit in each region. Dotted line: best fit up to $10^{18.5}$ eV.

Figure 2: Fly's Eye monocular differential energy spectrum multiplied by E^3. Points: data. Dashed line: best fit of the total spectrum. Dotted line: best fit up to $10^{18.5}$ eV.

Figure 3: X_{max} elongation rate. Black dots: Fly's Eye data. Open squares : proton X_{max} distribution based on QCD Pomeron model. Open circles: iron X_{max} distribution based on QCD Pomeron model. Diamonds: expected mean X_{max} distribution based on a simple two component assumption of cosmic rays.

Figure 4: Two component fit to the stereo Fly's Eye energy spectrum. Points: data. Dotted lines: best fit in each region. Dashed lines: two individual components. Diamonds: superposition of the two components.

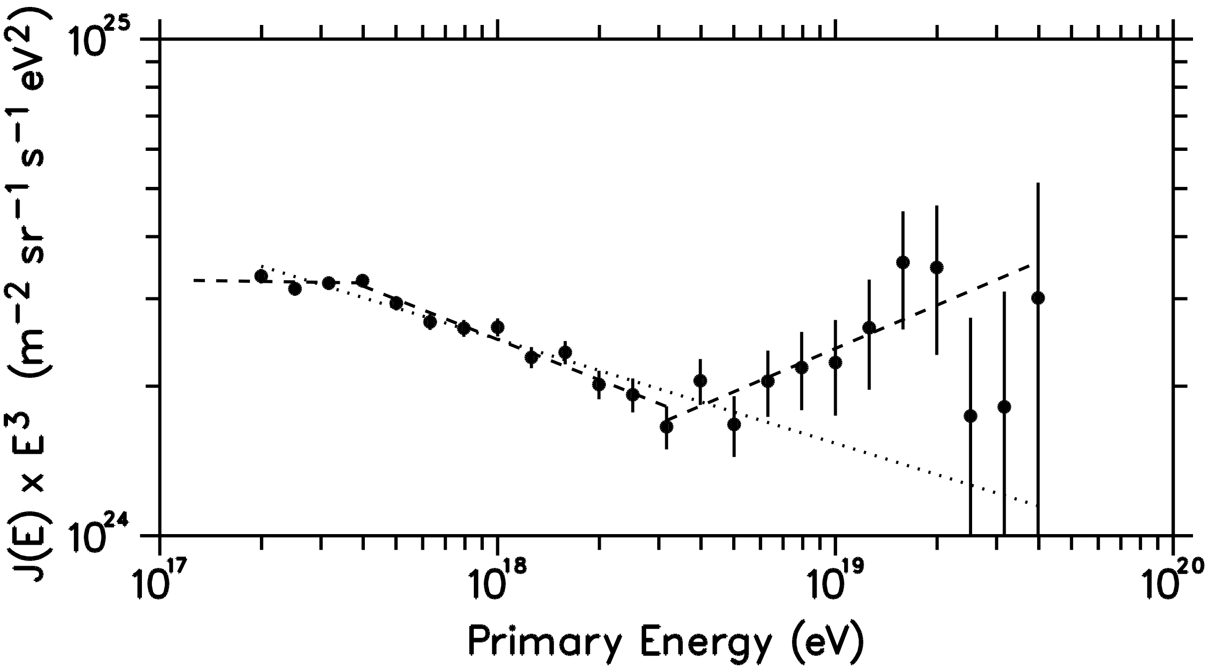

Figure 1: Fly's Eye stereo energy spectrum. Points: data. Dashed line: best fit in each region. Dotted line: best fit up to $10^{18.5}$ eV.

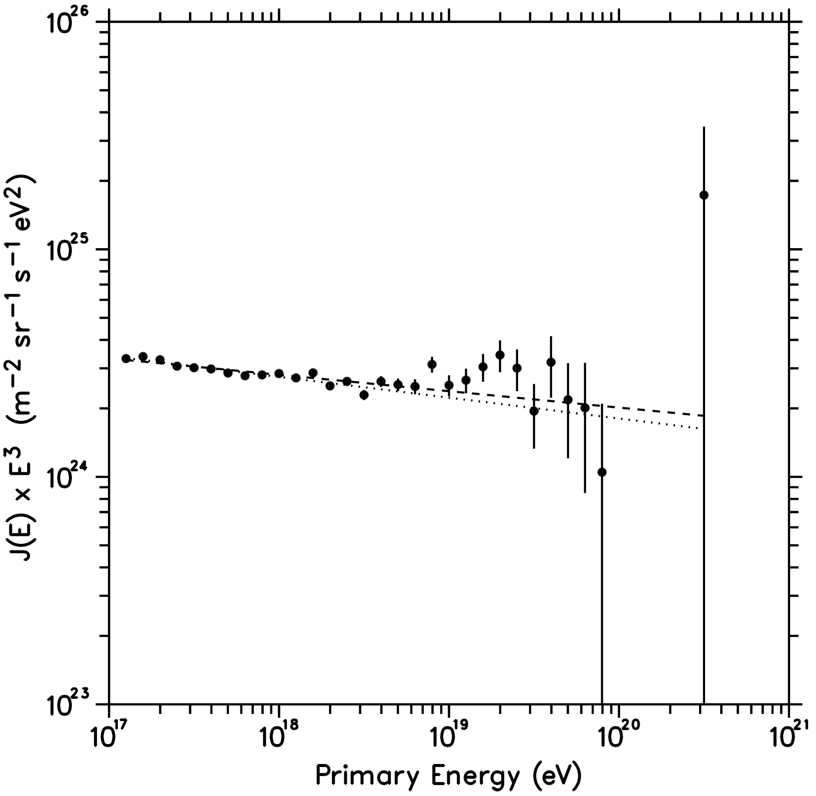

Figure 2: Fly's Eye monocular energy spectrum. Points: data. Dashed line: best fit of the total spectrum. Dotted line: best fit up to $10^{18.5}$ eV.

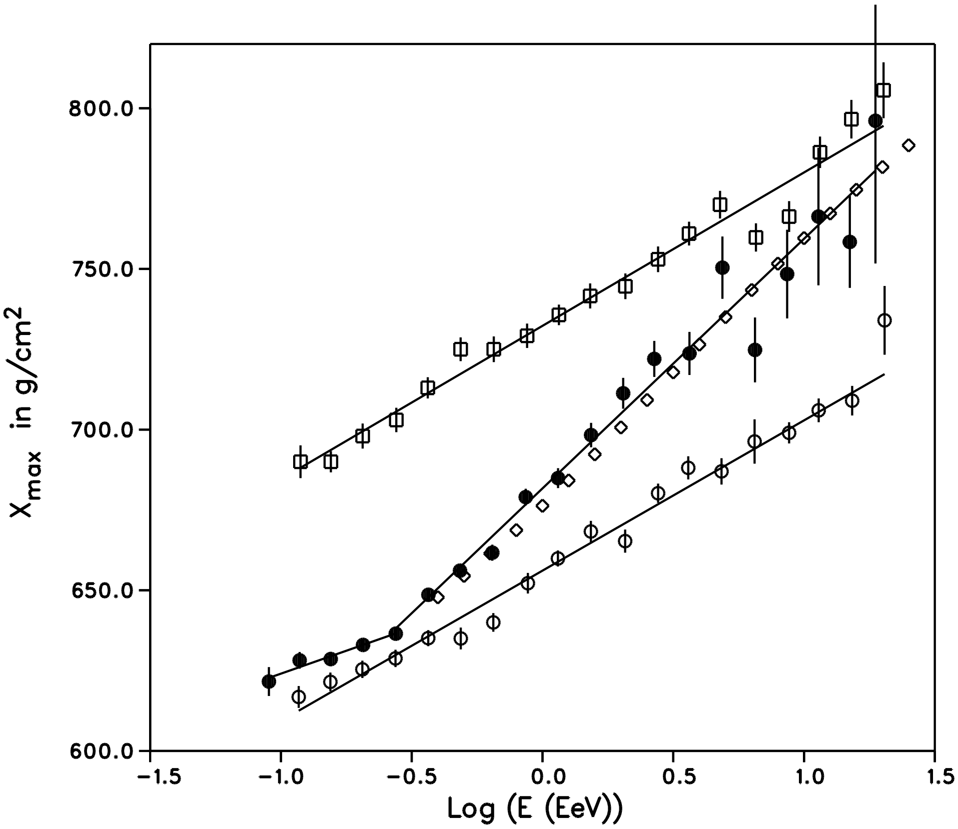

Figure 3: X_{max} elongation rate. Black dots: Fly's Eye data. Open squares : proton X_{max} distribution based on QCD Pomeron model. Open circles: iron X_{max} distribution based on QCD Pomeron model. Diamonds: expected mean X_{max} distribution based on a simple two component assumption of cosmic rays.

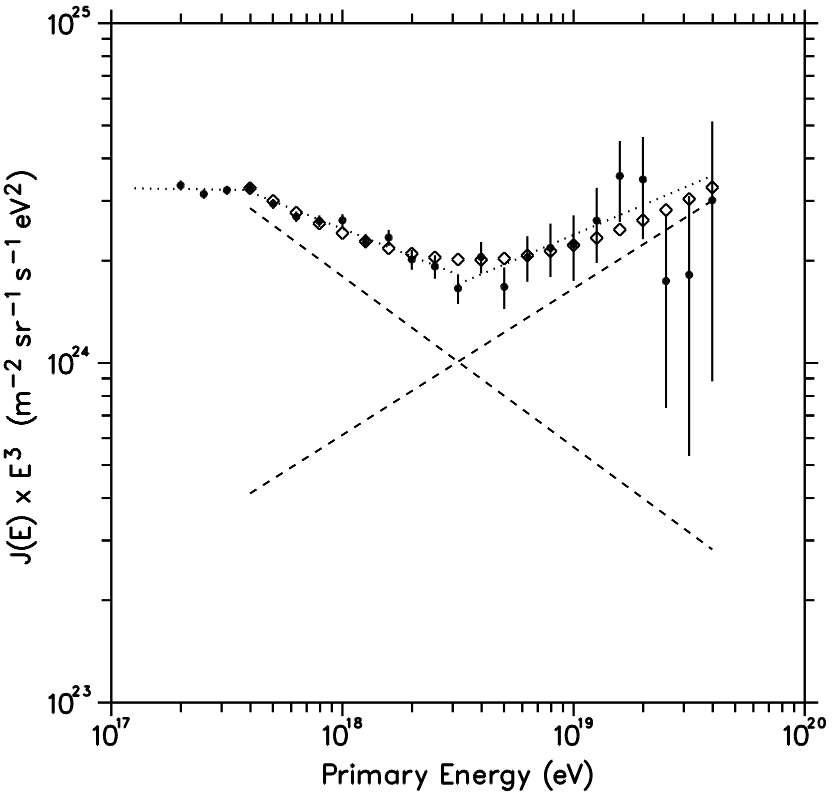

Figure 4: Figure 4: Two component fit to the stereo Fly's Eye energy spectrum. Points: data. Dotted lines: best fit in each region. Dashed lines: two individual components. Diamonds: superposition of the two components.